Vol. 44 — N° 3 09 20 P. 581 – 591

GEOSTANDARDS and GEOANALYTICAL RESEARCH

# Development of Iron Speciation Reference Materials for Palaeoredox Analysis

Lewis J. **Alcott** (1)†, Alexander J. **Krause** (1)†, Emma U. **Hammarlund** (2), Christian J. **Bjerrum** (3), Florian **Scholz** (4), Yijun **Xiong** (1), Andrew J. **Hobson** (1), Lesley **Neve** (1), Benjamin J.W. **Mills** (1), Christian **März** (1), Bernhard **Schnetger** (5), Andrey **Bekker** (6) and Simon W. **Poulton** (1)*

(1) School of Earth and Environment, University of Leeds, Leeds, LS2 9JT, UK
(2) Translational Cancer Research, Lund University, Lund 223 63, Sweden
(3) Department of Geosciences and Natural Resource Management, Section of Geology, University of Copenhagen, Copenhagen 1350, Denmark
(4) GEOMAR Helmholtz Centre for Ocean Research Kiel, Wischhofstraße 1–3, Kiel 24111, Germany
(5) ICBM, University of Oldenburg, Carl-von-Ossietzky-Strasse, Oldenburg 26123, Germany
(6) Department of Earth and Planetary Sciences, University of California, Riverside, CA 92521, USA
* Corresponding author. e-mail: s.poulton@leeds.ac.uk
† Joint first authors.

**The development and application of geochemical techniques to identify redox conditions in modern and ancient aquatic environments has intensified over recent years. Iron (Fe) speciation has emerged as one of the most widely used procedures to distinguish different redox regimes in both the water column and sediments, and is the main technique used to identify oxic, ferruginous (anoxic, Fe(II) containing) and euxinic (anoxic, sulfidic) water column conditions. However, an international sediment reference material has never been developed. This has led to concern over the consistency of results published by the many laboratories that now utilise the technique. Here, we report an interlaboratory comparison of four Fe speciation reference materials for palaeoredox analysis, which span a range of compositions and reflect deposition under different redox conditions. We provide an update of extraction techniques used in Fe speciation and assess the effects of both test portion mass, and the use of different analytical procedures, on the quantification of different Fe fractions in sedimentary rocks. While atomic absorption spectroscopy and inductively coupled plasma-optical emission spectrometry produced comparable Fe measurements for all extraction stages, the use of ferrozine consistently underestimated Fe in the extraction step targeting mixed ferrous–ferric minerals such as magnetite. We therefore suggest that the use of ferrozine is discontinued for this Fe pool. Finally, we report the combined data of four independent Fe speciation laboratories to characterise the Fe speciation composition of the reference materials. These reference materials are available to the community to provide an essential validation of in-house Fe speciation measurements.**

Keywords: iron speciation, sequential extraction, reference materials, water column redox, total iron, ancient sediments.

**Received 04 Dec 19 – Accepted 22 Apr 20**

Tracking the chemical evolution of Earth's atmosphere and oceans has long been a topic of considerable interest, with much focus on the changing state of ocean redox chemistry throughout Earth history, including its connection to the rise of atmospheric oxygen and the evolution of the biosphere (e.g., Canfield 2005). Key to understanding Earth's past is the development and application of (bio)geochemical proxies to assess and track the redox state of the oceans. Currently used inorganic geochemical redox proxies include a variety of trace metal contents and ratios (e.g., Brumsack 2006, Robbins *et al.* 2016), rare earth element ratios (e.g., German and Elderfield 1990), molybdenum isotopes (e.g., Arnold *et al.* 2004), chromium isotopes (e.g., Frei *et al.* 2009), uranium isotopes (e.g., Weyer *et al.* 2008), Fe/Al ratios (e.g., Lyons and Severmann 2006, Clarkson *et al.* 2014) and Fe speciation (e.g., Poulton *et al.* 2004a, Poulton and Canfield 2005, 2011, Raiswell *et al.* 2018).

Iron speciation is a particularly well-established and widely used palaeoredox proxy for fine-grained siliciclastic

doi: 10.1111/ggr.12342

sediments. We present a brief overview of its evolution here and direct the reader to Raiswell *et al.* (2018) for a more detailed history of the proxy. Initially, the use of Fe speciation focussed on identifying controls on the formation of sedimentary pyrite ($Fe_{py}$), particularly the availability of reactive iron. This led to the development of the degree of pyritisation (DOP) parameter (Berner 1970):

$$DOP = Fe_{py}/(Fe_{py} + HCl\,soluble\,Fe) \quad (1)$$

Subsequently, the DOP method was calibrated to distinguish aerobic, restricted and inhospitable bottom waters (Raiswell *et al.* 1988, Raiswell and Al Biatty 1989), where $Fe_{py}$ was determined via the chromium reduction method (Canfield *et al.* 1986), and a 1 min boiling HCl extraction was used to define a 'reactive' Fe pool ($Fe_R$).

Further work on Fe minerals in modern marine sediments found that Fe-(oxyhydr)oxides are the dominant phases that react on early diagenetic timescales (Canfield 1989), with such minerals having half-lives with respect to their sulfidation of the order of minutes to tens of days (Canfield *et al.* 1992, Poulton *et al.* 2004b). However, while the boiling HCl extraction successfully extracts such minerals (Raiswell *et al.* 1994), it also extracts Fe from a variety of sheet silicate minerals (termed $Fe_{prs}$; poorly reactive silicates), which are only reactive towards dissolved sulfide on a million-year timescale (Raiswell and Canfield 1996). As a result, a sodium dithionite solution was developed (Canfield 1989, Raiswell *et al.* 1994) as a more suitable extractant of Fe (oxyhydr)oxide minerals (termed $Fe_{ox}$). Raiswell and Canfield (1998) then defined a 'highly reactive' Fe pool ($Fe_{HR}$) as the sum of $Fe_{ox}$ and $Fe_{py}$.

Canfield *et al.* (1996) observed that high ratios of $Fe_{HR}/Fe_T$ (normalisation to total Fe, $Fe_T$, is used to account for variable dilution by carbonate, organic matter or silica, as well as differences in grain size) commonly occur in sediments deposited beneath the euxinic water column of the Black Sea. This occurs due to the water column formation and settling of Fe sulfide minerals, which augments the terrestrial influx of $Fe_{HR}$ minerals. Extensive further studies of modern and ancient marine settings demonstrated that under anoxic water column conditions, $Fe_{HR}/Fe_T$ ratios commonly exceed 0.38, whereas values are generally below this for oxic depositional conditions (Canfield *et al.* 1996, Raiswell and Canfield 1998, Raiswell *et al.* 2001, Poulton and Raiswell 2002).

Under ferruginous water column conditions, sedimentary $Fe_{HR}$ enrichments arise due to precipitation of non-sulfidised Fe minerals such as Fe-(oxyhydr)oxides (e.g., Sun *et al.* 2015), green rust and magnetite (Zegeye *et al.* 2012), Fe carbonates (e.g., Jiang and Tosca 2019) or potentially Fe silicates (e.g., Rasmussen *et al.* 2015). Recognising that magnetite and Fe carbonate minerals such as siderite were not extracted by existing techniques, Poulton and Canfield (2005) further refined the iron speciation methodology. This resulted in the development of a sequential extraction procedure to determine magnetite ($Fe_{mag}$) and iron-carbonate ($Fe_{carb}$) minerals, in addition to the previously identified $Fe_{ox}$, $Fe_{py}$ and $Fe_{prs}$ pools (with FeHR calculated as the sum of $Fe_{carb}$, $Fe_{ox}$, $Fe_{mag}$ and $Fe_{py}$).

Based on observations from the Black Sea (Anderson and Raiswell 2004), Poulton *et al.* (2004a) developed the utility of Fe speciation further, by utilising the $Fe_{py}/Fe_{HR}$ ratio to distinguish euxinic (sulfidic) and ferruginous (containing dissolved $Fe^{2+}$) depositional conditions. In addition, noting that rapid deposition of terrigenous sediment and/or transfer of $Fe_{HR}$ to $Fe_{prs}$ under anoxic non-sulfidic conditions can both decrease depositional $Fe_{HR}/Fe_T$ ratios (to potentially give a false oxic signal under anoxic depositional conditions), Poulton and Canfield (2011) revised the calibration boundaries. Thus, oxic depositional conditions are now commonly recognised by $Fe_{HR}/Fe_T < 0.22$, ferruginous conditions are characterised by $Fe_{HR}/Fe_T > 0.38$ and $Fe_{py}/Fe_{HR} < 0.7$–$0.8$, and euxinic conditions are characterised by $Fe_{HR}/Fe_T > 0.38$ and $Fe_{py}/Fe_{HR} > 0.7$–$0.8$. When $Fe_{HR}/Fe_T$ ratios are between 0.22 and 0.38, an 'equivocal' zone is recognised, where additional consideration is required to evaluate water column redox conditions. In particular, $Fe_{prs}$ concentrations and $Fe_{prs}/Fe_T$ ratios (Poulton *et al.* 2010, Cumming *et al.* 2013, Doyle *et al.* 2018), and Fe/Al ratios (Lyons and Severmann *et al.* 2006, Clarkson *et al.* 2014) may be used to identify whether transfer of $Fe_{HR}$ to $Fe_{prs}$ has lowered initial depositional $Fe_{HR}$ concentrations.

As a consequence of these developments, the iron speciation scheme of Poulton and Canfield (2005) has become widely used for evaluating palaeoredox depositional conditions. However, while individual laboratories commonly use their own in-house reference materials as a procedural check, there is concern that discrepancies in operational procedures across different laboratories may be producing inconsistent results. Consequently, there is a clear requirement for a set of international reference materials. Here, we report the development of four reference materials for assessing ancient water column redox conditions via Fe speciation. This is based on the results of four independent laboratories, including the laboratories of the authors who developed and calibrated

the Fe speciation technique that is now widely used (Poulton and Canfield 2005). We additionally present details of the methodology applied and discuss operational issues related to the technique.

## Experimental procedure

### Samples

Four marine shale samples (WHIT, KL133, KL134 and BHW) were selected to encompass a range of iron phase compositions, depositional settings and periods of Earth history. WHIT was collected from the Mulgrave Shale Member of the Whitby Mudstone Formation at Saltwick Bay, Whitby, UK (Simms *et al.* 2004). The sample is early Jurassic (Toarcian; ~ 183 Ma) in age (Simms *et al.* 2004) and is a fine-grained, laminated, organic carbon-rich mudstone thought to have been deposited in an anoxic water column (Wignall *et al.* 2005). KL133 and KL134 were collected from well-preserved drill core (borehole KL1/65) at the National Core Library, Donkerhoek, South Africa. These two Late Permian (Catuneanu *et al.* 2005, Branch *et al.* 2007) samples are from below and above the occurrence of the Upper Ecca microfloras of the Ecca and Beaufort Groups (Linol *et al.* 2016, Chere *et al.* 2017). KL133 (1025 m depth in core KL1/65) is from just beneath the Upper Ecca microflora and is comprised of grey-black silty shale (Linol *et al.* 2016). KL134 (104 m depth in core KL1/65) is a light-grey siltstone from above the microfloras (Linol *et al.* 2016). While there is ongoing debate as to the absolute ages of the Ecca and Beaufort Groups, the two samples were deposited at ~ 265 Ma (e.g., McKay *et al.* 2015, Linol *et al.* 2016). BHW is a partially silicified, dolomitic black shale of the Archaean (~ 2.6 Ga) Black Reef Quartzite Formation, Transvaal Supergroup. The sample was taken from well-preserved drill core (62.5 m depth in core BHW-289) stored at the National Core Library, Donkerhoek, South Africa.

### Sample preparation and storage

Post-collection, weathered surfaces were removed and rocks were crushed at the University of Leeds using an agate TEMA pulverising mill, to obtain powder with the consistency of flour and without any larger isolated mineral grains. Initial attempts to sieve several of the samples were found to be problematic, due to coagulation of clay minerals during the procedure, which prevented adequate sieving and altered the nature of the sieved sediment. Thus, to ensure homogeneity of each entire bulk sample, powders were well-mixed via the repetitive use of a v-splitter, before decantation into acid-clean jars containing ~ 100 g of rock powder. For longer term storage, samples are preserved under a nitrogen atmosphere at a constant temperature of 20 °C to prevent sample oxidation. For short-term storage, we recommend that samples are kept in a desiccator, either under vacuum or under an anaerobic atmosphere, to minimise potential oxidation and to retain a low moisture content (Kane and Potts 2007).

### Organic carbon analyses

Total organic carbon (TOC) was determined at the University of Leeds. Samples ($n$ = 12 for each reference material) of approximately 0.5 g were initially decarbonated with 10 ml of 20% *v/v* HCl for one hour. This was performed in 15 ml centrifuge tubes, which were left open to allow for $CO_2$ degassing. After centrifugation, the supernatant was decanted, and samples were then treated with a further 10 ml of 20% *v/v* HCl, followed by constant shaking at room temperature for 16 h. Following this, the supernatant was decanted, and 10 ml of high-purity water (from a Milli-Q® system, Molsheim, France) was added to the samples and agitated for 30 min. The samples were then repeatedly washed with high-purity water until the supernatant reached pH > 4. The samples were then left to dry overnight, and TOC was measured using a LECO carbon–sulfur analyser, with LECO's certified carbon soil used as an internal reference material. This internal reference material had a recovery of 101.03% TOC and a reproducibility (RSD) of 1.60% ($n$ = 8).

### Major element determinations

Major element determinations were performed at the University of Oldenburg and the University of Leeds using wavelength dispersive X-ray fluorescence spectrometry. At ICBM, borate glass beads were produced by fusing 0.7 g of sample with 4.2 g of $Li_2B_4O_7$, following a peroxidation procedure with 1.0 g of $(NH_4)_2NO_3$ in a platinum crucible. Samples were then analysed using a Panalytical AxiosmAX spectrometer. At the University of Leeds, glass beads were created by fusing 0.4 g of sample with 4 g of flux (66% $Li_2B_4O_7$ + 34% $LiBO_2$) and two drops of lithium iodide solution (250 g $l^{-1}$) in a platinum crucible, and samples were measured using a Rigaku ZSX Primus II spectrometer. Calibration, including line overlap correction and matrix correction, was based on international reference samples (66, ICBM; 70, University of Leeds). Accuracy was checked by international and in-house reference materials not included in the calibration, with an error for major elements of < 6% at ICBM and < 3% at the University of Leeds. Measurement precision was < 1% for major elements.

## Iron extractions

All iron extractions were conducted under oxic conditions using Analytical Reagent grade chemicals, and each analyst performed a batch of eight replicates of each extraction. The sequential extractions and pyrite dissolutions were performed at four independent Fe speciation laboratories, including the Cohen Laboratory at the University of Leeds (three different analysts), the NordCEE Laboratory at the University of Southern Denmark, the Sediment and Aqueous Geochemistry Laboratory at the University of Copenhagen, and the Marine Geosystems Laboratory at the GEOMAR Helmholtz Centre for Ocean Research. The broad target phases for each extraction are reported in Table 1. However, it should be noted that these are operationally defined extractions, and the Fe speciation technique for palaeoredox analysis is predicated on the reactivity of different Fe pools towards dissolved sulfide, rather than the quantification of specific Fe minerals, which is a common misconception. Thus, the precise minerals extracted in each step (and the extent of their dissolution) will vary dependent on mineral crystallinity (see Raiswell *et al.* 1994) and a host of other factors, including impurities within the structure (see Poulton *et al.* 2004b). However, the Fe dissolved in each extraction can be considered to comprise an iron pool of similar reactivity towards dissolved sulfide, and it is this factor that has been calibrated in the use of Fe speciation as a palaeoredox indicator.

The sequential iron extractions (steps a–c; Table 1) were performed with a standard test portion mass of 60 ± 10 mg (accurately weighed), but tests were also performed using a test portion of up to 100 mg. Extraction solutions were prepared at room temperature, and the extractant volume for each step was 10 ml. During extractions, samples were constantly agitated (either horizontally on a shaking table or via an overhead shaker) in 15 ml centrifuge tubes as occasional shaking was found to result in incomplete extraction of the Fe phases. For step (a) at 50 °C, samples were shaken either on a heated shaking table, or on a conventional shaking table placed in an oven. Between extraction steps, samples were centrifuged prior to decanting and analysis.

**Table 1.**
**Summary of iron speciation methods and their target phases**

| Method | Target phase | Terminology |
|---|---|---|
| Ia) Na acetate, pH 4.5, 48 h, 50 °C | Carbonate Fe, including siderite and ankerite | $Fe_{carb}$ |
| Ib) Dithionite, 2 h | Ferric oxides, including ferrihydrite, haematite and goethite | $Fe_{ox}$ |
| Ic) Oxalate, 6 h | Magnetite Fe | $Fe_{mag}$ |
| II) Chromous chloride | Pyrite Fe | $Fe_{py}$ |
| III) Boiling concentrated HCl | Reactive Fe, poorly reactive sheet silicate Fe | $Fe_R$, $Fe_{prs}$ |
| IV) XRF | Total Fe, unreactive silicate Fe | $Fe_T$, $Fe_U$ |

Steps Ia–Ic were performed sequentially. An unreactive Fe fraction ($Fe_U$) can be calculated as the difference between $Fe_T$ and the sum of $Fe_{carb}$ + $Fe_{ox}$ + $Fe_{mag}$ + $Fe_{py}$ + $Fe_{prs}$.

**(a) Sodium acetate:** Samples were subjected to 10 ml of a 1 mol $l^{-1}$ sodium acetate solution buffered with acetic acid (pH = 4.5) for 48 h, at a constant temperature of 50 °C. Carbonate-poor samples were degassed 1 h after the addition of sodium acetate and again after 6 h. Carbonate-rich samples were degassed 1, 2, 6 and 24 h after sodium acetate addition. This first step ($Fe_{carb}$) primarily targets iron associated with carbonate phases (Table 1).

**(b) Sodium dithionite:** The sample was then treated with 10 ml of a sodium dithionite solution (50 g $l^{-1}$ sodium dithionite, 58.82 g $l^{-1}$ tri-sodium citrate, 20 ml $l^{-1}$ acetic acid) for 2 h. The sodium dithionite solution was always prepared immediately prior to use, to avoid oxidation of the solution and hence a lower extraction potential. This step ($Fe_{ox}$) primarily targets ferric oxide minerals (Table 1).

**(c) Ammonium oxalate:** The final step of the sequential iron extraction targets mixed ferric/ferrous oxides, such as magnetite ($Fe_{mag}$). This was achieved with 10 ml of a 0.2 mol $l^{-1}$ ammonium oxalate/0.17 mol $l^{-1}$ oxalic acid solution, with a treatment time of 6 h.

**(d) Hot chromous chloride distillation:** This method dissolves sulfide minerals, primarily comprising acid-volatile sulfides (AVS) and pyrite ($Fe_{py}$; Canfield *et al.* 1986). The amount of sample required for this method depends on the amount of sulfide present. For the WHIT, reference sample ~ 0.2 g was used for the extraction, for KL133 and KL134 ~ 2.5 g was used, and for BHW ~ 1.75 g was used. These sample masses ensure a sufficient amount of $Ag_2S$ precipitation for later quantification. The samples were initially treated with near-boiling 50% *v/v* HCl (8 ml) under a nitrogen atmosphere to test for the presence of AVS (Canfield *et al.* 1986). However, no AVS was detected in any of the samples, and thus, after addition of the HCl, 16 ml of chromous chloride was added. This solution was boiled for 1 h, also under a nitrogen atmosphere, and the released hydrogen sulfide was trapped (as $Ag_2S$) in a 1 mol $l^{-1}$ $AgNO_3$ solution (with additional $AgNO_3$ added where appropriate to avoid saturation of the trap with sulfide). The

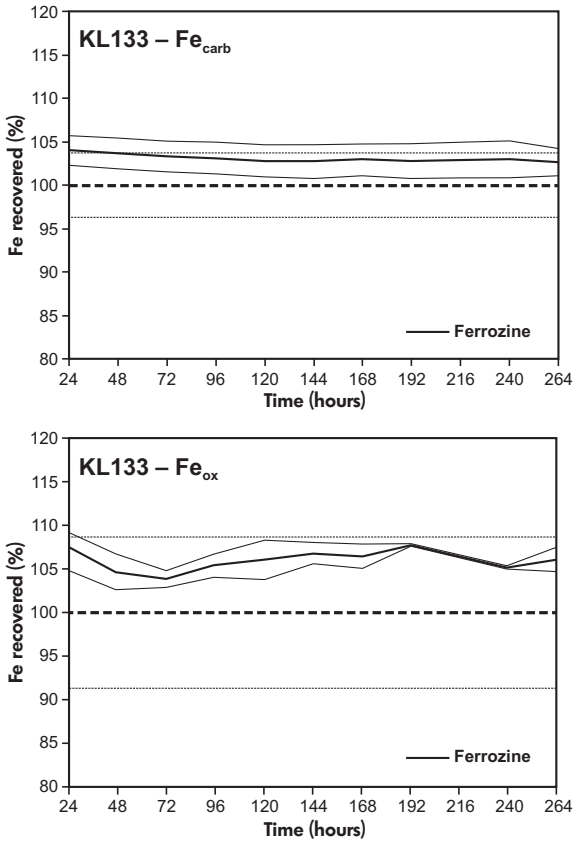


**Figure 1. Recovery of Fe for KL133 (solid line ± 1*s*) in the $Fe_{carb}$ and $Fe_{ox}$ fractions, as determined by the spectrophotometric ferrozine method, relative to the mean combined value determined via AAS and ICP-OES (dashed line ± 1*s*).**

$Ag_2S$ precipitates were then filtered, dried and weighed, and the concentration of pyrite Fe was determined stoichiometrically. In one of the laboratories, Zn acetate was used to trap the released $H_2S$ instead of $AgNO_3$, and sulfide analysis was performed by spectrophotometry using diamine reagent (Cline 1969).

**(e) Concentrated HCl:** To determine $Fe_R$, approximately 100 mg of sample was weighed into a glass test tube. Concentrated HCl (5 ml) was added, and the sample was immediately gently heated for 60 s to bring to the boil. The sample was then boiled more aggressively for a further 60 s (Berner 1970, Raiswell *et al.* 1994). Samples were then immediately quenched with high-purity water and transferred quantitatively to 100 ml volumetric flasks and made up to volume. The difference between $Fe_R$ and the sum of $Fe_{carb}$ + $Fe_{ox}$ + $Fe_{mag}$ gives $Fe_{prs}$. Note, however, that this extraction may also be performed sequentially after steps Ia–Ic (Table 1), which gives a direct measurement of $Fe_{prs}$ without the need to subtract $Fe_{carb}$, $Fe_{ox}$ and $Fe_{mag}$ (Poulton and Canfield 2005).

## Analysis of Fe solutions

Three commonly used techniques were compared for the analysis of the Fe solutions from steps a–c and e. Atomic absorption spectrometry (AAS) was the primary technique used by three of the laboratories. In this case, for the sequential extraction steps a–c, the supernatant was subjected to a twenty times dilution with high-purity water prior to analysis relative to matrix-matched reference materials. The same procedure was used for boiling HCl extractions, but with a five times dilution of the initial 100 ml solution. The fourth laboratory determined dissolved Fe via inductively coupled plasma-optical emission spectroscopy (ICP-OES). Here, solutions were diluted forty-fold with 1% *v/v* $HNO_3$. The dilution acid contained 10 μg $g^{-1}$ yttrium as an internal standard element, which was monitored to compensate for matrix-related signal fluctuation.

Finally, we tested the utility of the ferrozine method (Stookey 1970). Here, we used the approach of Sperling *et al.* (2013), whereby 100 μl of extract was added to 4 ml of solution (prepared immediately prior to analysis) containing 12 g $l^{-1}$ HEPES buffer, 0.2 g $l^{-1}$ ferrozine reagent and 10 g $l^{-1}$ hydroxylamine hydrochloride (which reduces Fe(III)

Table 2.
**Mean (± 1*s*) major element mass fractions of reference materials (expressed as % *m/m*), measured by two independent XRF laboratories**

| RM | Si | | Ti | | Al | | Fe | | Mn | | Mg | | Ca | | Na | | K | | P | |
|---|---|---|---|---|---|---|---|---|---|---|---|---|---|---|---|---|---|---|---|---|
| | Mean | 1*s* | Mean | 1*s* | Mean | 1*s* | Mean | 1*s* | Mean | 1*s* | Mean | 1*s* | Mean | 1*s* | Mean | 1*s* | Mean | 1*s* | Mean | 1*s* |
| WHIT | 22.74 | 0.24 | 0.553 | 0.009 | 11.9 | 0.16 | 4.54 | 0.02 | 0.019 | 0.001 | 1.10 | 0.02 | 1.03 | 0.02 | 0.378 | 0.009 | 2.65 | 0.02 | 0.070 | 0.003 |
| KL133 | 31.06 | 0.19 | 0.371 | 0.007 | 7.81 | 0.03 | 3.19 | 0.03 | 0.065 | 0.001 | 1.44 | 0.04 | 0.970 | 0.016 | 1.18 | 0.03 | 3.13 | 0.04 | 0.083 | 0.002 |
| KL134 | 28.49 | 0.83 | 0.385 | 0.007 | 8.87 | 0.25 | 5.03 | 0.07 | 0.087 | 0.002 | 1.00 | 0.04 | 0.652 | 0.008 | 1.60 | 0.08 | 2.66 | 0.04 | 0.092 | 0.003 |
| BHW | 32.75 | 0.33 | 0.236 | 0.009 | 7.48 | 0.06 | 1.62 | 0.02 | 0.017 | 0.001 | 1.03 | 0.03 | 0.100 | 0.010 | 0.065 | 0.004 | 6.88 | 0.09 | 0.018 | 0.003 |

Table 3.
Mean mass fractions (± 1*s*) of Fe in each sequential Fe extraction (% *m/m*), as determined by AAS, ICP-OES and spectrophotometry

| ID | $Fe_{carb}$ | | | $Fe_{ox}$ | | | $Fe_{mag}$ | | |
|---|---|---|---|---|---|---|---|---|---|
| | Mean | 1*s* | % RSD | Mean | 1*s* | % RSD | Mean | 1*s* | % RSD |
| **WHIT** | | | | | | | | | |
| AAS | 0.581 | 0.033 | 5.7 | 0.063 | 0.010 | 15.9 | 0.106 | 0.012 | 11.3 |
| ICP-OES | 0.593 | 0.009 | 1.5 | 0.058 | 0.002 | 3.5 | 0.081 | 0.002 | 2.5 |
| Spec. | 0.616 | 0.008 | 1.3 | 0.084 | 0.001 | 1.6 | 0.106 | 0.003 | 2.8 |
| **KL133** | | | | | | | | | |
| AAS | 0.139 | 0.006 | 4.3 | 0.046 | 0.004 | 8.7 | 0.169 | 0.011 | 6.5 |
| ICP-OES | 0.139 | 0.004 | 2.9 | 0.046 | 0.002 | 4.3 | 0.157 | 0.010 | 6.4 |
| Spec. | 0.145 | 0.002 | 1.4 | 0.049 | 0.001 | 2.0 | 0.149 | 0.003 | 2.0 |
| **KL134** | | | | | | | | | |
| AAS | 0.711 | 0.041 | 5.8 | 0.095 | 0.010 | 10.5 | 0.584 | 0.028 | 4.8 |
| ICP-OES | 0.680 | 0.020 | 2.9 | 0.088 | 0.003 | 3.4 | 0.532 | 0.016 | 3.0 |
| Spec. | 0.781 | 0.005 | 0.6 | 0.110 | 0.001 | 0.9 | 0.538 | 0.012 | 2.2 |
| **BHW** | | | | | | | | | |
| AAS | 0.044 | 0.006 | 13.6 | 0.016 | 0.003 | 18.8 | 0.024 | 0.002 | 8.3 |
| ICP-OES | 0.044 | 0.002 | 4.5 | 0.018 | 0.003 | 16.7 | 0.023 | 0.005 | 21.7 |
| Spec. | 0.045 | 0.001 | 2.2 | 0.015 | 0.001 | 6.7 | 0.020 | 0.001 | 5.0 |

Spectrophotometry data are reported after 24 h for $Fe_{carb}$ and Feox, and after 168 h for $Fe_{mag}$ (see text for further details).

to Fe(II), to allow measurement by ferrozine). At the same time, a range of matrix-matched reference materials was prepared. For these reference materials, we compared the results of using both an Fe(III) stock solution (1000 μg $ml^{-1}$ Fe $(NO_3)_3$ in 0.5 mol $l^{-1}$ $HNO_3$) and an Fe(II) stock solution (Mohr's salt, $(NH_4)_2Fe(SO_4)_2.6H_2O$). For the $Fe_{carb}$ and $Fe_{ox}$ extractions, similar results were obtained using both stock Fe solutions. However, for the $Fe_{mag}$ extraction, a precipitate formed when using the Fe(II) stock solution, and thus, all of our results are reported relative to reference materials prepared with the Fe(III) stock solution. Sperling *et al.* (2013) left samples overnight to allow colour development, followed by analysis by spectrophotometer. To further test this technique, we performed regular repeat measurements of the solutions and reference materials (on a Genesys 6 spectrophotometer, Thermo Scientific, Massachusetts, USA) for up to 16 days after preparation.

## Results and discussion

### Bulk geochemical characterisation

Replicate TOC analyses ($n = 12$) produced mean values of 2.63 ± 0.03% *m/m* for WHIT, 0.09 ± 0.03% *m/m* for KL133, 0.85 ± 0.05% *m/m* for KL134 and 0.29 ± 0.03% *m/m* for BHW. Measurement results for major elements are shown in Table 2. We stress here that we include major element determinations to provide context for our samples. The major element determinations provided in Table 2 do not represent officially certified mass fractions and should not be viewed as such. A high degree of reproducibility is observed for all samples, and of particular significance, $Fe_T$ mass fractions show a relatively wide range across the four reference materials, from 1.62% to 5.03% *m/m* (Table 2).

### Comparison of iron determinations in the extraction solutions by different techniques

A comparison of iron determinations by AAS, ICP-OES and spectrophotometry is presented in Table 3. The RSD for each measurement was generally within ~ 6%, with the exception of fractions with very low Fe contents where, as expected, RSDs are commonly higher. Nevertheless, despite these higher RSDs, the magnitude of the measured standard deviation is relatively small for the low Fe fractions (Table 3), and this degree of variability has little impact in terms of quantifying $Fe_{HR}/Fe_T$ and $Fe_{py}/Fe_{HR}$ ratios (see below). The RSD for AAS analyses is often higher than for the other measurement techniques, which likely reflects the fact that extractions for the solutions measured by AAS were performed by multiple users across three different laboratories, whereas extractions measured by ICP-OES and spectrophotometry were performed by one user in one laboratory.

In general, there is good agreement (within error) between the measurements by AAS and ICP-OES for all

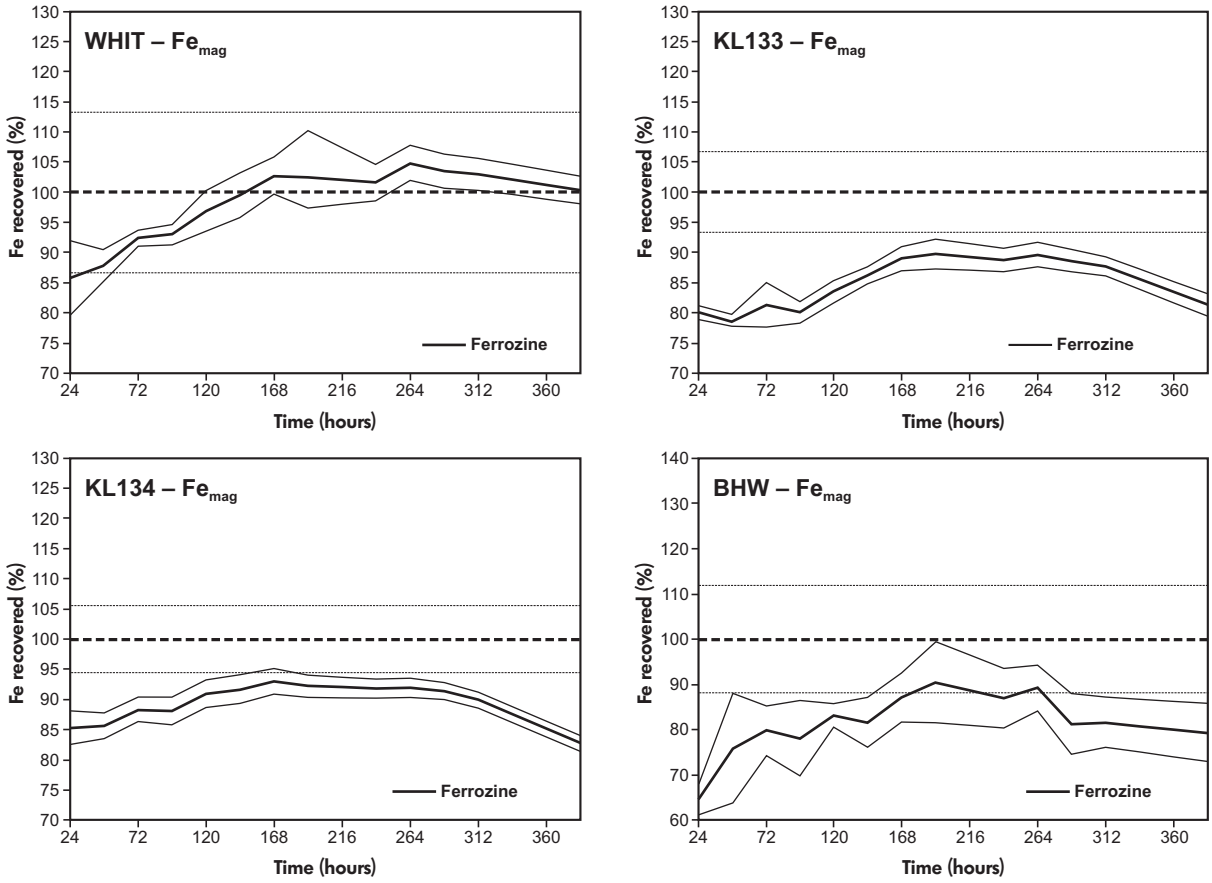


**Figure 2. Recovery of $Fe_{mag}$ for the four reference materials (solid line ± 1*s*), as determined by the spectrophotometric ferrozine method, relative to the mean combined value determined via AAS and ICP-OES (dashed line ± 1*s*).**

extracted phases (Table 3), highlighting that both techniques are suitable for measuring the sequential Fe solutions, despite the potential for strong matrix effects. In addition, we found that the ferrozine technique generally produced comparable results for $Fe_{carb}$ and $Fe_{ox}$ (Table 3), and this was a consistent feature across the 11 days over which these analyses were performed (Figure 1). However, while there is reasonable agreement between both the $Fe_{mag}$ AAS/ICP-OES analyses and the spectrophotometric analyses after around 7 days of ferrozine reaction (Table 3), after 24 h of reaction (the current standard technique is to leave solutions overnight prior to analysis) only ~ 60–85% of the $Fe_{mag}$ pool was measured by spectrophotometer (Figure 2). This suggests that the extracted Fe may be strongly complexed by the reagents in the oxalate extraction, such that considerable time is required for the reaction with ferrozine to proceed to completion. Furthermore, the mean spectrophotometric $Fe_{mag}$ results for KL133, KL134 and BHW were always lower than the mean value determined by AAS, with a distinct decrease to even lower values after ~ 11 days. We thus conclude that the ferrozine spectrophotometric technique is not suitable for the measurement of $Fe_{mag}$.

## Effect of test portion mass on sequential extraction efficiency

During the course of our analyses, we found that the initial test portion sample mass to extractant ratio may affect the quantity of Fe dissolved. To test this, we performed replicate extractions ($n$ = 4–8) for all four reference materials using three initial masses: 50, 70 and 100 mg, with Fe determined by ICP-OES. We found that lower concentrations were consistently obtained for $Fe_{carb}$ as sample mass increased (Table 4). By contrast, the subsequent $Fe_{ox}$ and $Fe_{mag}$ extractions showed no consistent trends as sample mass increased, and thus, the total amount of iron extracted during the three sequential phases decreased at higher sample masses (Table 1). We observed no consistent trend in the RSD of analyses over the range of sample masses used in our tests, even though in general, the relative

Table 4.
The effect of test portion mass on extraction efficiency. The sum of the three sequential extraction phases is also shown ($Fe_{carb}$ + $Fe_{ox}$ + $Fe_{mag}$)

| ID | $Fe_{carb}$ (% *m/m*) | | | $Fe_{ox}$ (% *m/m*) | | | $Fe_{mag}$ (% *m/m*) | | | Sum (% *m/m*) | | |
|---|---|---|---|---|---|---|---|---|---|---|---|---|
| | Mean | 1*s* | % RSD | Mean | 1*s* | % RSD | Mean | 1*s* | % RSD | Mean | 1*s* | % RSD |
| **WHIT** | | | | | | | | | | | | |
| 50 mg | 0.618 | 0.003 | 0.5 | 0.056 | 0.001 | 1.8 | 0.073 | 0.001 | 1.4 | 0.748 | 0.003 | 0.4 |
| 70 mg | 0.593 | 0.008 | 1.3 | 0.058 | 0.002 | 3.4 | 0.078 | 0.003 | 3.9 | 0.729 | 0.010 | 1.4 |
| 100 mg | 0.549 | 0.008 | 1.4 | 0.056 | 0.002 | 3.6 | 0.078 | 0.003 | 3.9 | 0.683 | 0.011 | 1.6 |
| **KL133** | | | | | | | | | | | | |
| 50 mg | 0.151 | 0.005 | 3.3 | 0.048 | 0.004 | 8.3 | 0.149 | 0.001 | 0.7 | 0.348 | 0.009 | 2.6 |
| 70 mg | 0.137 | 0.006 | 4.4 | 0.046 | 0.002 | 4.3 | 0.155 | 0.009 | 5.8 | 0.338 | 0.012 | 3.6 |
| 100 mg | 0.133 | 0.005 | 3.8 | 0.045 | 0.002 | 4.4 | 0.145 | 0.009 | 6.2 | 0.323 | 0.014 | 4.3 |
| **KL134** | | | | | | | | | | | | |
| 50 mg | 0.734 | 0.026 | 3.5 | 0.091 | 0.004 | 4.4 | 0.507 | 0.012 | 2.4 | 1.332 | 0.026 | 2.0 |
| 70 mg | 0.689 | 0.019 | 2.8 | 0.087 | 0.003 | 3.4 | 0.512 | 0.023 | 4.5 | 1.289 | 0.016 | 1.2 |
| 100 mg | 0.651 | 0.009 | 1.4 | 0.088 | 0.003 | 3.4 | 0.513 | 0.012 | 2.3 | 1.251 | 0.021 | 1.7 |
| **BHW** | | | | | | | | | | | | |
| 50 mg | 0.048 | 0.003 | 6.3 | 0.018 | 0.002 | 11.1 | 0.02 | 0.002 | 10.0 | 0.087 | 0.007 | 8.0 |
| 70 mg | 0.044 | 0.002 | 4.5 | 0.019 | 0.003 | 15.8 | 0.021 | 0.004 | 19.0 | 0.084 | 0.007 | 8.3 |
| 100 mg | 0.038 | 0.001 | 2.6 | 0.015 | 0.001 | 6.7 | 0.018 | 0.005 | 27.8 | 0.071 | 0.005 | 7.0 |

standard deviation would be expected to increase at lower sample masses. Based on these considerations, we propose an optimal sample mass for the sequential extractions of 60 ± 10 mg for 10 ml of extractant.

## Development of iron speciation reference materials

We utilise the replicate extractions (as measured by AAS and ICP-OES) of the six users from four independent laboratories to determine the Fe speciation characteristics of the four reference materials (Table 5). Concentrations of $Fe_{ox}$ are relatively low for all four samples, as might be expected for sediments that have experienced anaerobic conditions during early diagenesis (whereby dissimilatory iron reduction and reaction with dissolved sulfide both result in the reductive dissolution of Fe-(oxyhydr)oxides), but the remaining Fe pools show considerable variability. In addition, mean poorly reactive sheet silicate Fe mass fractions (calculated as $Fe_{prs} = Fe_R - (Fe_{carb} + Fe_{ox} + Fe_{mag})$) are 0.219% *m/m* for WHIT, 1.399% *m/m* for KL133, 2.283% *m/m* for KL134 and 0.462% *m/m* for BHW. This gives $Fe_{prs}/Fe_T$ ratios of 0.05 for WHIT, 0.44 for KL133, 0.45 for KL134 and 0.29 for BHW. The $Fe_{prs}/Fe_T$ ratio for WHIT is low compared with the mean ratio for Phanerozoic shales (0.39 ± 0.11; Raiswell *et al.* 2008), but the remaining samples fall close to this mean.

In Figure 3, we plot $Fe_{HR}/Fe_T$ and $Fe_{py}/Fe_{HR}$ ratios for each reference material (see Table 5), and we show the standard deviations that are obtained as a result of propagating the precision of measurements for each Fe pool through to the calculation of Fe speciation ratios. This demonstrates that the determination of Fe speciation ratios is highly reproducible, with the largest degree of variability occurring for the BHW $Fe_{py}/Fe_{HR}$ ratio, which arises due to

Table 5.
Mean mass fractions (% *m/m* ± 1*s*) of Fe in each fraction, and $Fe_{HR}/Fe_T$ and $Fe_{py}/Fe_{HR}$ ratios (± 1*s*) for each reference material

| ID | $Fe_{carb}$ | | $Fe_{ox}$ | | $Fe_{mag}$ | | $Fe_{py}$ | | $Fe_R$ | | $Fe_{HR}/Fe_T$ | | $Fe_{py}/Fe_{HR}$ | |
|---|---|---|---|---|---|---|---|---|---|---|---|---|---|---|
| | Mean | 1*s* | Mean | 1*s* | Mean | 1*s* | Mean | 1*s* | Mean | 1*s* | Mean | 1*s* | Mean | 1*s* |
| WHIT | 0.583 | 0.030 | 0.062 | 0.009 | 0.103 | 0.014 | 1.970 | 0.087 | 0.967 | 0.097 | 0.60 | 0.02 | 0.73 | 0.04 |
| KL133 | 0.139 | 0.005 | 0.046 | 0.004 | 0.167 | 0.011 | 0.011 | 0.002 | 1.751 | 0.121 | 0.11 | 0.00 | 0.03 | 0.01 |
| KL134 | 0.705 | 0.039 | 0.094 | 0.009 | 0.578 | 0.032 | 0.011 | 0.002 | 3.660 | 0.124 | 0.28 | 0.01 | 0.01 | 0.00 |
| BHW | 0.044 | 0.005 | 0.017 | 0.003 | 0.023 | 0.003 | 0.068 | 0.008 | 0.546 | 0.077 | 0.09 | 0.01 | 0.45 | 0.06 |

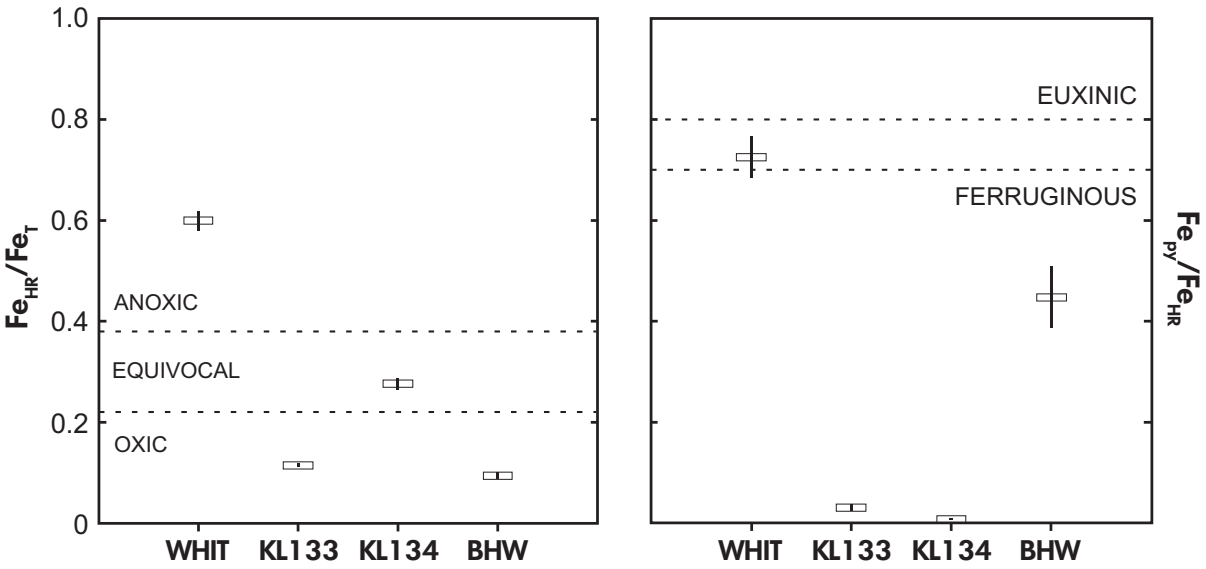


**Figure 3. Iron speciation characteristics of the reference materials. Range bars are calculated based on the propagation of standard deviations (1*s*) determined for individual extractions.**

the low concentration of each Fe fraction in this sample (Table 5). The reference materials also document a range of redox conditions, including oxic (KL133, BHW), equivocal (KL134) and anoxic (WHIT). $Fe_{py}/Fe_{HR}$ ratios are only relevant as a water column redox indicator for samples that show clear evidence of deposition under anoxic water column conditions (Poulton and Canfield 2011), and the anoxic WHIT sample plots close to the threshold for identifying euxinia. The remaining reference materials have variable $Fe_{py}/Fe_{HR}$ ratios, which likely reflect different levels of sulfide production during diagenesis. Taken together, the variable speciation characteristics, combined with the wide range of mass fractions evident across the Fe fractions, suggest that these four samples are ideal as international reference materials.

## Conclusions

We have developed four reference materials that may be used by researchers conducting Fe speciation analyses of palaeodepositional redox conditions. In the process of creating these reference materials, we have refined 'best practice' techniques for Fe speciation analyses, including detailed evaluation of the commonly employed techniques for determining Fe mass fractions in extracted solutions. The amount of iron dissolved in each extraction step is sensitive to both sample agitation and test portion mass, and we recommend that extractions are performed with a test portion mass of 60 ± 10 mg for 10 ml of extractant. In addition, we recommend that the spectrophotometric determination of $Fe_{mag}$ by ferrozine is discontinued.

The reference materials comprise a range of Fe fraction mass fractions and document a range of depositional redox conditions. In addition, Fe mass fractions and speciation ratios are generally highly reproducible, with a greater degree of uncertainty being limited to those fractions containing very low mass fractions of Fe. These characteristics confirm the wide-ranging suitability of the samples as international reference materials for iron speciation analyses. The samples are stored under controlled conditions, where oxygen, light and moisture are eliminated, making them suitable as long-term reference materials for the community.

## Acknowledgements

LJA. is funded by a Leeds Anniversary Research Scholarship. AJK. is funded by a studentship from the NERC SPHERES Doctoral Training Partnership (NE/L002574/1). CJB acknowledges support from DONG Energy (now INEOS Oil & Gas Denmark) and GeoCenter Denmark. FS thanks the German Research Foundation (DFG) for financial support through Emmy Noether Nachwuchsforschergruppe ICONOX. SWP. acknowledges support from a Leverhulme Research Fellowship and a Royal Society Wolfson Research Merit Award. Lewis J. Alcott and Alexander J. Krause are joint first authors.

## Data availability statement

Data supporting this study are available on request from the authors.

## References


**Anderson T.F. and Raiswell R. (2004)**
Sources and mechanisms for the enrichment of highly reactive iron in euxinic Black Sea sediments. American Journal of Science, 304, 203–233.

**Arnold G.L., Anbar A.D., Barling J. and Lyons T.W. (2004)**
Molybdenum isotope evidence for widespread anoxia in Mid-Proterozoic oceans. Science, 304, 87–90.

**Berner R.A. (1970)**
Sedimentary pyrite formation. American Journal of Science, 268, 1–23.

**Branch T., Ritter O., Weckman U., Scachsenhofer R. and Schilling F. (2007)**
The Whitehill Formation – A high conductivity marker horizon in the Karoo Basin. South African Journal of Geology, 110, 465–476.

**Brumsack H.J. (2006)**
The trace metal content of recent organic carbon-rich sediments: Implications for Cretaceous black shale formation. Palaeogeography, Palaeoclimatology, Palaeoecology, 232, 344–361.

**Canfield D.E., Raiswell R., Westrich J.T., Reaves C.M. and Berner R.A. (1986)**
The use of chromium reduction in the analysis of reduced inorganic sulfur in sediments and shales. Chemical Geology, 54, 149–155.

**Canfield D.E., Raiswell R. and Bottrell S.H. (1992)**
The reactivity of sedimentary iron minerals towards sulfide. American Journal of Science, 292, 659–683.

**Canfield D.E., Lyons T.W. and Raiswell R. (1996)**
A model for iron deposition to euxinic Black Sea sediments. American Journal of Science, 296, 818–834.

**Canfield D.E. (1989)**
Reactive iron in marine sediments. Geochimica et Cosmochimica Acta, 53, 619–632.

**Canfield D.E. (2005)**
The early history of atmospheric oxygen: Homage to Robert M. Garrels. Annual Review of Earth and Planetary Sciences, 33, 1–36.

**Catuneanu O., Wopfner H., Eriksson P.G., Carincross B., Rubidge B.S., Smith R.M.H. and Hancox J.P. (2005)**
The Karoo Basins of south-central Africa. Journal of African Earth Sciences, 43, 211–253.

**Chere N., Linol B., de Wit M. and Schulz H.-M. (2017)**
Lateral and temporal variations of black shales across the southern Karoo Basin – Implications for shale gas exploration. South African Journal of Geology, 120, 541–564.

**Clarkson M.O., Poulton S.W., Guilbaud R. and Wood R.A. (2014)**
Assessing the utility of Fe/Al and Fe-speciation to record water column redox conditions in carbonate-rich sediments. Chemical Geology, 382, 111–122.

**Cline J.D. (1969)**
Spectrophotometric determination of hydrogen sulfide in natural waters. Limnology and Oceanography, 14, 454–458.

**Cumming V.M., Poulton S.W., Rooney A.D. and Selby D. (2013)**
Anoxia in the terrestrial environment during the late Mesoproterozoic. Geology, 41, 583–586.

**Doyle K.A., Poulton S.W., Newton R.J., Podkovyrov V.N. and Bekker A. (2018)**
Shallow water anoxia in the Mesoproterozoic ocean: Evidence from the Bashkir Meganticlinorium, Southern Urals. Precambrian Research, 317, 196–210.

**Frei R., Gaucher C., Poulton S.W. and Canfield D.E. (2009)**
Fluctuations in Precambrian atmospheric oxygenation recorded by chromium isotopes. Nature, 461, 250–253.

**German C.R. and Elderfield H. (1990)**
Application of the Co anomaly as a paleoredox indicator: The ground rules. Paleoceanography, 5, 823–833.

**Jiang C.Z. and Tosca N.J. (2019)**
Fe(II)-carbonate precipitation kinetics and the chemistry of anoxic ferruginous seawater. Earth and Planetary Science Letters, 506, 231–242.

**Kane J.S. and Potts P.J. (2007)**
ISO best practices in reference material certification and use in geoanalysis. Geostandards and Geoanalytical Research, 31, 361–378.

**Linol B., Chere N., Muedi T., Nengovhela V. and de Wit M.J. (2016)**
Deep borehole lithostratigraphy and basin structure of the Southern Karoo basin re-visited. In: Linol B. and de Wit M.J. (eds), Origin and evolution of the Cape Mountains and Karoo Basin. Springer (Switzerland), 3–15.

**Lyons T.W. and Severmann S. (2006)**
A critical look at iron paleoredox proxies: New insights from modern euxinic marine basins. Geochimica et Cosmochimica Acta, 70, 5698–5722.

**McKay M.P., Weislogel A.L., Fildani A., Brunt R.L., Hodgson D.M. and Flint S.S. (2015)**
U-Pb zircon tuff geochronology from the Karoo Basin, South Africa: Implications of zircon recycling on stratigraphic age controls. International Geology Review, 57, 393–410.

**Poulton S.W. and Raiswell R. (2002)**
The low-temperature geochemical cycle of iron: From continental fluxes to marine sediment deposition. American Journal of Science, 302, 774–805.

**Poulton S.W., Fralick P.W. and Canfield D.E. (2004a)**
The transition to a sulphidic ocean ~ 1.84 billion years ago. Nature, 431, 173–177.

## references


**Poulton S.W., Krom M.D. and Raiswell R. (2004b)**
A revised scheme for the reactivity of iron (oxyhydr)oxide minerals towards dissolved sulfide. Geochimica et Cosmochimica Acta, 68, 3703–3715.

**Poulton S.W. and Canfield D.E. (2005)**
Development of a sequential extraction procedure for iron: Implications for iron partitioning in continentally derived particulates. Chemical Geology, 214, 209–221.

**Poulton S.W., Fralick P.W. and Canfield D.E. (2010)**
Spatial variability in oceanic redox structure 1.8 billion years ago. Nature Geoscience, 3, 486–490.

**Poulton S.W. and Canfield D.E. (2011)**
Ferruginous conditions: A dominant feature of the ocean through Earth's history. Elements, 7, 107–112.

**Raiswell R., Buckley F., Berner R.A. and Anderson T.F. (1988)**
Degree of pyritization of iron as a paleoenvironmental indicator of bottom-water oxygenation. Journal of Sedimentary Petrology, 58, 812–819.

**Raiswell R., Canfield D.E. and Berner R.A. (1994)**
A comparison of iron extraction methods for the determination of degree of pyritization and the recognition of iron-limited pyrite formation. Chemical Geology, 111, 101–110.

**Raiswell R. and Canfield D.E. (1996)**
Rates of reaction between silicate iron and dissolved sulfide in Peru Margin sediments. Geochimica et Cosmochimica Acta, 60, 2777–2787.

**Raiswell R. and Canfield D.E. (1998)**
Sources of iron for pyrite formation in marine sediments. American Journal of Science, 298, 219–245.

**Raiswell R. and Al Biatty H.J. (1989)**
Depositional and diagenetic C-S-Fe signatures in early Palaeozoic normal marine shales. Geochimica et Cosmochimica Acta, 53, 1147–1152.

**Raiswell R., Newton R. and Wignall P.B. (2001)**
An indicator of water-column anoxia: Resolution of biofacies variations in the Kimmeridge Clay (Upper Jurassic, UK). Journal of Sedimentary Research, 71, 286–294.

**Raiswell R., Newton R., Bottrell S.H., Coburn P.M., Briggs D.E.G., Bond D.P.G. and Poulton S.W. (2008)**
Turbidite depositional influences on the diagenesis of Beecher's Trilobite Bed and the Hunsrück Slate: Sites of soft tissue pyritization. American Journal of Science, 308, 105–129.

**Raiswell R., Hardisty D., Lyons T.W., Canfield D.E., Owens J.D., Planavsky N.J., Poulton S.W. and Reinhard C.T. (2018)**
The iron paleoredox proxies: A guide to the pitfalls, problems and proper practice. American Journal of Science, 318, 491–526.

**Rasmussen B., Krapez B., Muhling J.R. and Suvorova A. (2015)**
Precipitation of iron silicate nanoparticles in early Precambrian oceans marks Earth's first iron age. Geology, 43, 303–306.

**Robbins L.J., Lalonde S.V., Planavsky N.J., Partin C.A., Reinhard C.T., Kendall B., Scott C., Hardisty D.S., Gill B.C., Alessi D.S., Dupont C.L., Saito M.A., Crowe S.A., Poulton S.W., Bekker A., Lyons T.W. and Konhauser K.O. (2016)**
Trace elements at the intersection of marine biological and geochemical evolution. Earth-Science Reviews, 163, 323–348.

**Simms M.J., Chidlaw N., Morton N. and Page K.N. (2004)**
British Lower Jurassic stratigraphy. Geological Conservation Review Series, No. 30, Joint Nature Conservation Committee (Peterborough, UK), 458pp.

**Sperling E.A., Halverson G.P., Knoll A.H., Macdonald F.A. and Johnston D.T. (2013)**
A basin redox transect at the dawn of animal life. Earth and Planetary Science Letters, 371, 143–155.

**Stookey L.L. (1970)**
Ferrozine – A new spectrophotometric reagent for iron. Analytical Chemistry, 42, 779–781.

**Sun S., Konhauser K.O., Kappler A. and Li Y.-L. (2015)**
Primary hematite in Neoarchean to Paleoproterozoic oceans. Geological Society of America Bulletin, 127, 850–861.

**Weyer S., Anbar A.D., Gerdes A., Gordon G.W., Algeo T.J. and Boyle E.A. (2008)**
Natural fractionation of $^{238}U/^{235}U$. Geochimica et Cosmochimica Acta, 72, 345–359.

**Wignall P.B., Newton R.J. and Little C.T.S. (2005)**
The timing of paleoenvironmental change and cause-and-effect relationships during the early Jurassic mass extinction in Europe. American Journal of Science, 305, 1014–1032.

**Zegeye A., Bonneville S., Benning L.G., Sturm A., Fowle D.A., Jones C., Canfield D.E., Ruby C., MacLean L.C., Nomosatryo S., Crowe S.A. and Poulton S.W. (2012)**
Green rust formation controls nutrient availability in a ferruginous water column. Geology, 40, 599–602.